Med Chem Res (2014) 23:1581–1590
DOI 10.1007/s00044-013-0739-5

MEDICINAL CHEMISTRY RESEARCH

ORIGINAL RESEARCH

Theoretical studies, synthesis, and biological activity of 1-[(4-methylphenyl)sulfonyl]-5-oxo-2,3,4,5-tetrahydro-1*H*-1-benzazepine-4-carbonitrile (C9) as a non-peptide antagonist of the arginine vasopressin V1a and V2 receptors

M. Citlalli Contreras-Romo · José Correa-Basurto · Itzia Padilla-Martínez · Marlet Martínez-Archundia · Federico Martínez-Ramos · Magdalena J. Ślusarz · Gilberto López-Pérez · Andrés Quintanar-Stephano

Received: 21 March 2013 / Accepted: 17 August 2013 / Published online: 4 September 2013

Abstract In this work, the synthesis of 1-[(4-methylphenyl)sulfonyl]-5-oxo-2,3,4,5-tetrahydro-1*H*-1-benzazepine-4-carbonitrile (**C9**) and the study of its biological activity as a new putative antagonist of vasopressin receptors are described. The chemical identification of the compound **C9** was confirmed using ^{1}H and ^{13}C nuclear magnetic resonance. This compound contains a moiety core similar to those of vaptans; therefore, we decided to study the compound's binding on vasopressin receptors (V1aR and V2R), whose models were built, refined by molecular dynamics simulations, and validated through docking studies. The biological effects of **C9** on vascular smooth muscle (VSM) contractility and aquaresis were also tested. Rat aortic rings were used to test the inhibitory effect of **C9** (0.0, 5.9, 59, and 590 μM) on AVP-induced VSM contraction (10 μM). The inhibition of the antidiuretic effect of vasopressin (50 μU/kg) by **C9** (100 μg/kg) was determined using a water load test in rats. The results showed that **C9** inhibits aortic rings' contraction in a concentration-dependent manner, whereas **C9** exhibited an aquaretic effect on urine flow. Docking studies showed that **C9** reaches the vaptan binding site via the V1a and V2 receptors, which explains the similarity in their biological effects. The results indicate that **C9** functions as an antagonist on both V1aR and V2R.

Keywords
1-[(4-Methyl phenyl)sulfonyl]-5-oxo-2,3,4,5-tetrahydro-1*H*-1-benzazepine-4-carbonitrile · Vaptans · Docking · Molecular dynamic · Vasopressin · Vasopressin receptors

M. C. Contreras-Romo · A. Quintanar-Stephano (✉)
Departamento de Fisiología y Farmacología, Centro de Ciencias Básicas, Universidad Autónoma de Aguascalientes, Av. Universidad 940, Cd. Universitaria, 20131 Aguascalientes, Ags., Mexico
e-mail: aquinta@correo.uaa.mx

M. C. Contreras-Romo
e-mail: citlallicr@hotmail.com

J. Correa-Basurto · M. Martínez-Archundia
Laboratorio de Modelado Molecular y Bioinformática, Sección de Estudios de Posgrado e Investigación, Escuela Superior de Medicina, Instituto Politécnico Nacional, Plan de San Luis y Díaz Mirón, 11340 Mexico City, Mexico
e-mail: corrjose@gmail.com.mx

J. Correa-Basurto · G. López-Pérez
Laboratorio de Bioqímica, Sección de Estudios de Posgrado e Investigación, Escuela Superior de Medicina, Instituto Politécnico Nacional, Plan de San Luis y Díaz Mirón, 11340 Mexico City, Mexico

I. Padilla-Martínez
Unidad Profesional Interdisciplinaria de Biotecnología del Instituto Politécnico Nacional, Av. Acueducto s/n, Barrio la Laguna Ticomán, 07340 Mexico City, DF, Mexico
e-mail: ipadillamar@ipn.mx

F. Martínez-Ramos
Laboratorio de Investigación, Departamento de Química Inorgánica, Escuela Nacional de Ciencias Biológicas, IPN., Prolongación de Carpio y Plan de Ayala S/N, DF, Mexico
e-mail: licomartin20@gmail.com

M. J. Ślusarz
Faculty of Chemistry, University of Gdańsk, Sobieskiego 18, 80-952 Gdańsk, Poland
e-mail: magda@chem.univ.gda.pl

Introduction

Arginine vasopressin (AVP), a nonapeptide synthesized in the magnocellular neurosecretory cells of the supraoptic and paraventricular nuclei of the hypothalamus, is transported via the pituitary stalk to the posterior pituitary, where it is stored and released into the blood. The main function of AVP is to regulate the body water balance using a homeostatic mechanism (Hardman and Limbird, 2001; Guyton and Hall, 1999). Abnormal increases in AVP secretion occur in congestive heart failure (CHF), liver cirrhosis, ascites, kidney diseases, syndrome of inappropriate antidiuretic hormone secretion (SIADH), and hyponatremia (Mah and Hofbauer, 1987; Laszlo *et al.*, 1991; Thibonnier *et al.*, 2002). Current treatments for these disorders include fluid restriction and hypertonic saline solution administration, either alone or with loop diuretics. However, one of the limitations of this treatment is its reduced effectiveness, mainly in patients with SIADH, who experience high volumes of water retention. In addition, hypertonic saline solution is poorly tolerated by patients with advanced CHF or overt congestion (Goldsmith, 2005). It is important to mention that currently there is no reliable, effective, and safe therapy for these diseases. Thus, the development of aquaretic drugs that promote the formation of diluted urine, concurrent with a low loss of electrolytes, is highly desirable.

Since the synthesis of AVP by du Vigneaud *et al.* (1954), many efforts have been undertaken to discover effective antagonists of AVP receptors. Interestingly, during in vivo studies on Brattleboro rats, it was found that these peptide antagonists act as partial agonists to AVP (Yamamura *et al.*, 1992). Recent studies based on computational tools, including molecular modeling, molecular docking, and quantitative structure–activity relationship (QSAR), have allowed the design of a new class of non-peptide drugs, which are ultimately synthetic substances that possess antagonistic properties to AVP receptors (AVPRs) (Giełdoń *et al.*, 2001; Czaplewski *et al.*, 1998; Mouillac *et al.*, 1995). These non-peptide AVPR antagonists (called vaptans) are orally and intravenously active (Jackson, 2006), and only a few of these AVPR antagonists have been used to treat patients. Furthermore, in animal experiments, low non-therapeutic doses of Conivaptan to pregnant rats induced adverse effects on the fetuses (Tahara *et al.*, 1997). Conivaptan is also a potent inhibitor of CYP3A4, which is primarily responsible for the metabolism of many drugs and may be the cause of unwanted drug interactions in protracted treatments. It was also found that at higher doses, Conivaptan increases the incidence of adverse effects, mainly hypotension and thirst (Zeltser *et al.*, 2007).

Therefore, it remains important to develop new drugs with improved aquaretic effects, but fewer side effects. In a previous work (Contreras-Romo *et al.*, submitted), we found that through in silico procedures, the benzoazepine group is the key moiety for the recognition of the vaptans into the AVP V1a and V2 receptors' binding pocket. In addition, the chemical structure of the **C9** contains the benzoazepine core. Based on this observations, we could hypothesize that **C9** can have biological effects as AVP V1a and V2 receptors' antagonist. Thus, the aim of this work was to synthesize the compound **C9** and test its potential biological activity as a blocker of the V1a and V2 receptors by evaluating VSM contractility and urine flow. The experimental work was supported by theoretical studies of molecular dynamics (MD) and docking simulations (see results).

Materials and methods

Melting points were measured in an Electrothermal 9300 apparatus and are uncorrected. IR spectra were recorded using a MIDAC M2000 FT-IR instrument (KBr). ^{1}H and ^{13}C-NMR spectra were recorded on a Varian Mercury 300 MHz (^{1}H, 300.08; ^{13}C, 75.46 MHz). The spectra were measured with tetramethylsilane as an internal reference while following standard techniques.

Adult male Wistar rats weighing 350–450 g each and originating from the Universidad Autónoma of Aguascalientes colony were used. The animal room was under controlled temperatures (22–24 °C) and light–dark conditions (lights on between 0700 and 1900 h). The diet consisted of Purina rat chow (Agribrands-Purina, México) and tap water ad libitum. All experimental procedures were approved by the Institutional Animal Care and Use Committee of the Universidad Autónoma of Aguascalientes, which are compatible with the ILAR (USA) guidelines, 1996.

Theoretical studies

Molecular dynamics (MD) simulations of V1aR and V2R

The AVP receptors, V1a and V2 were modeled using the I-TASSER program (Zhang, 2008) which employs an ab initio procedure due to the lack of knowing GPCR template close to 30 % of identity. The V1aR model shows a disulfide bridge between **C124** and **C203**, which is in agreement with the literature data (Barberis and Durroux, 1998). However, the V2R model shows a disulfide bridge between **C11** and **C192** (Schwieger *et al.*, 2008). Three-dimensional (3-D) models of these receptors were refined through MD simulations using the NAMD2.6 program

(Philips *et al.*, 2005), which utilizes all hydrogen topology, CHARMM22 (MacKerell *et al.*, 1998) for proteins, CHARMM27 (MacKerell *et al.*, 1998) for lipids, and the TIP3P model for water molecules.

Protein structures were solvated using the *solvate* plug-in syntax included in the visual molecular dynamics (VMD) program (Humphrey *et al.*, 1996), followed by the removal of unwanted water molecules located in the hydrophobic protein–membrane interface. In both cases, a POPC lipid bilayer was built using VMD (90×90 Å^{-2}). Finally, overlapping lipids were removed and the entire system was neutralized with an ionic concentration of 0.4 M NaCl, in accordance with the NAMD membrane tutorial.

MD simulations were conducted for approximately 15 ns at 310 K for both vasopressin receptors. The temperature was maintained using Langevin dynamics (Martyna *et al.*, 1994). Simulations were performed using a 2-fs time step, with the Shake algorithm for hydrogen atoms (Ryckaert *et al.*, 1977) and a multiple stepping algorithm to compute long-range electrostatic interactions, as depicted in the NAMD-program membrane tutorial. Force field parameters for non-bonded interactions were set as follows: cutoff (12 Å), switchdist (10 Å), and pairlistdist (13.5 Å). Periodic boundary conditions in conjunction with Particle Mesh Ewald (PME) were applied to calculate the full electrostatic energy of the unit cell. According to the root-mean square deviation (RMSD) analysis, the structure of V1aR reached stability after 5 ns (Fig. 1a). The V2R structure reached it at 3 ns (Fig. 2a). The RMSF analysis for V1aR revealed deviations around 6 Å in both the extracellular and intracellular loops, as well as in its amino

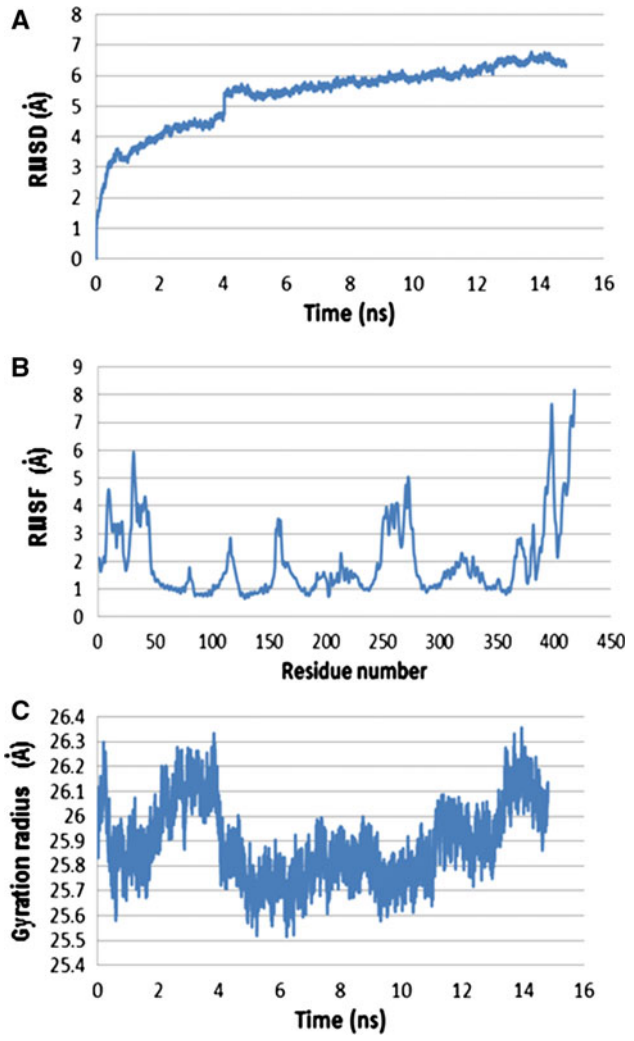

Fig. 1 V1aR MD simulations: **a** RMSD plots of the 8 ns MD simulations. **b** RMSF values showing greater movements in the loops. **c** R_g values show the compactness of the protein

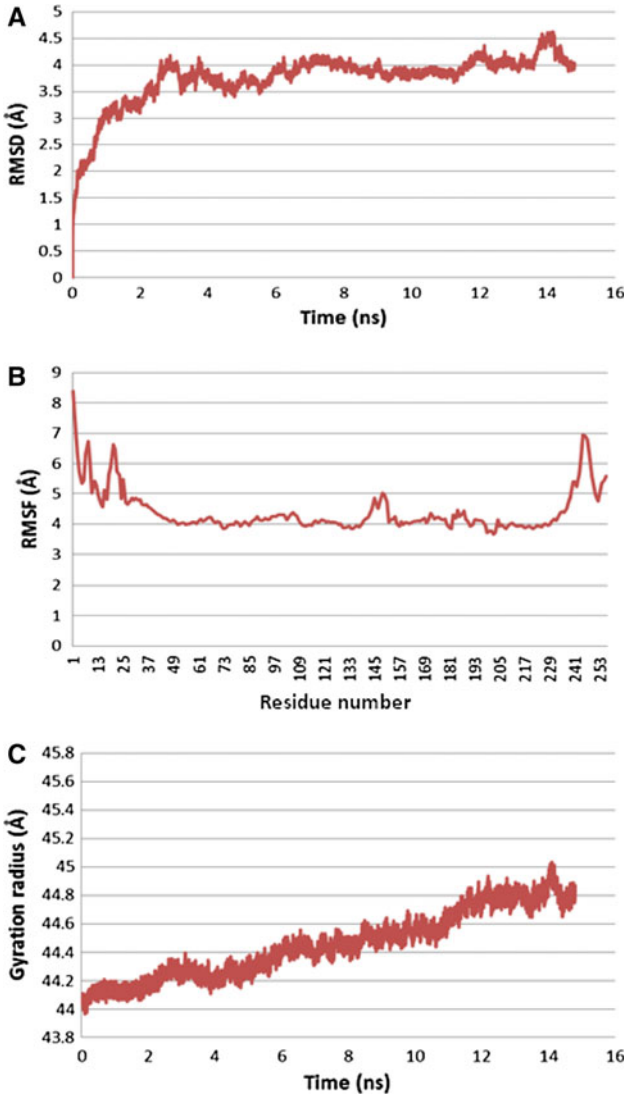

Fig. 2 V2R MD simulations: **a** RMSD plots of the 8 ns MD simulations. **b** RMSF values showing greater movements in the loops. **c** R_g values show the compactness of the protein

and carboxy terminal segments, whereas the transmembrane domains remained stable around 2 Å throughout the stimulation (Fig. 1b). The majority of V2R residues fluctuate approximately 4 Å, whereas the connecting loops did not show significant peaks compared to V1aR (Fig. 2b). The gyration radius (R_g) study on V1aR showed that the protein oscillated between 25.5 and 26.3 Å, with the major changes occurring before 4 ns (Fig. 1c). The V2R exhibited a significantly greater expansion throughout the trajectory, with R_g values around 44 Å (Fig. 2c).

Docking studies

Docking studies are used to identify important residues involved in ligand–receptor binding (Soriano-Ursúa *et al.*, 2010). The MD simulations were performed to refine the 3-D models of the V1a and V2 receptors. Furthermore, several snapshots were taken to obtain the best conformer of each receptor for use in the docking studies with **C9**. The docking studies on different vasopressin conformers (5 ns each in duration) allowed us to choose the best docking binding pose, in a manner similar to that reported by Giełdoń *et al.* (2001) for Conivaptan (Giełdoń *et al.*, 2001).

Docking studies were performed using Autodock 4.0.1 (Morris *et al.*, 1998). In the docking simulation studies, a grid box was defined as $40 \times 40 \times 40$ Å^{-3} and centered on the alpha carbon of V217 for V1a and alpha carbon of V206 for V2R. These amino acid residues were located in the center of the box that made contact with the Conivaptan (Giełdoń *et al.*, 2001). The spacing between grid points was 0.375 Å. Docking simulations were performed using the hybrid Lamarckian Genetic Algorithm with an initial population of 100 randomly placed individuals and a maximum number of energy evaluations of 1×10^7 (Morris *et al.*, 1998).

The docking studies allowed us to determine the binding free energy of **C9** into vasopressin receptors: −8.47 kcal/mol for V1aR and −5.76 kcal/mol for V2R. Moreover, the results showed that **C9** interacted with the following V1aR residues: T206, F207, P318, R214, S314, V217, Y216, S213, F189, G212, and W211 (Fig. 7); whereas that for the V2R, **C9** interacted with these: W200, P199, Q180, Q174, I209, Y124, M123, F287, Q291, and A294 (Fig. 8). These bindings were owing to the π–π interactions, π–cation and hydrogen bonds.

Chemical synthesis

Figure 3 shows the general synthetic pathway for **C9** compound.

*Methyl 2-{[(4-methylphenyl)sulfonyl]amino}benzoate (**2**)*

4-Methylbenzenesulfonyl chloride (3.77 g, 19.8 mmol) was added to a solution of methyl 2-aminobenzoate **1** (2.60 g, 17.2 mmol) in pyridine (5.20 g) at an internal temperature of 0 °C. The reaction mixture was warmed to 25 °C and stirred for 11 h. Water at 5 °C was poured into the mixture and stirred for 1 h; it was then cooled for 12 h to 5–10 °C. The resulting crystals were isolated by filtration and dried to yield **2** as a pale yellow powder. mp: 111 °C. Yield = 82.2 %. ^{1}H NMR (300 MHz, DMSO-d_6): δ 2.28 (3H, s), 3.64 (H, s), 7.12–7.82 (8H, m), 10.43 (1H, br s). IR (KBr): 3445, 3134, 2361, 1690 cm^{-1}. ^{13}C NMR (75 MHz, DMSO-d_6): δ 21.59, 53.33, 118.13, 120.3, 124.49, 127.64, 130.55, 131.70, 135.17, 136.30, 139.44, 144.79, 168.32.

*Methyl 2-{(3-cyanopropyl)[(4-methylphenyl) sulfonyl]amino}benzoate (**3**)*

A mixture of *N*-tosyl benzoate (**2**) (2.04 g, 6.68 mmol), 4-chlorobutanenitrile (0.815 g, 7.87 mmol), potassium carbonate (1.83 g, 13.2 mmol), and potassium iodide (0.326 g, 1.96 mmol) in 2-butanone (3.06 g) was stirred at reflux for 12 h. The mixture was then poured into cold

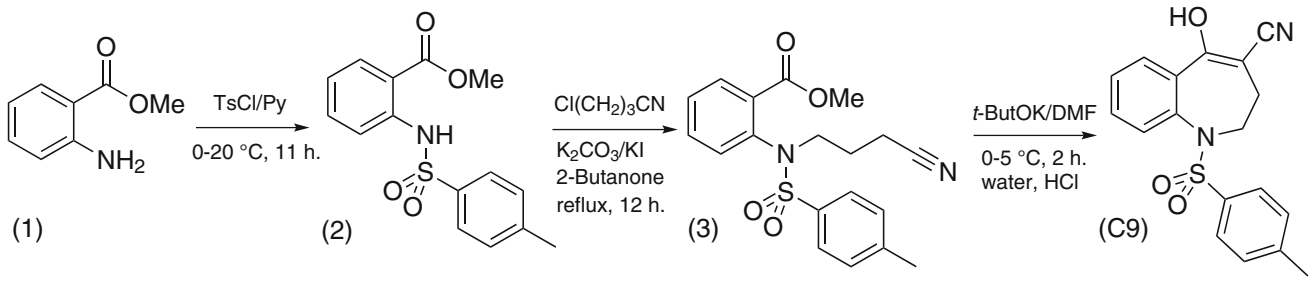

Fig. 3 Synthetic pathway to 1-[(4-methyl phenyl)sulfonyl]-5-oxo-2,3,4,5-tetrahydro-1*H*-1-benzazepine-4-carbonitrile (**C9**). Modified from Tsunoda *et al.* (2004)

water at 0–5 °C and stirred for 1 h. The resulting crystals were isolated by filtration and dried to provide **3** as a white powder. mp: 112 °C. Yield = 80.1 %. ^{1}H NMR (300 MHz, DMSO-d_6): δ 1.71 (2H, t), 2.36 (3H, s), 2.63 (2H, t), 3.48 (2H, s), 3.76 (H, s), 6.90–7.76 (8H, m). IR (KBr): 3440, 2935, 2241, 1732 cm^{-1}. ^{13}C NMR (75 MHz, DMSO-d_6): δ 14.23, 21.67, 24.86, 50.04, 52.81, 120.99, 127.88, 129.04, 129.19, 130.47, 131.27, 133.14, 133.36, 135.28, 137.83, 144.36, 167.03.

*1-[(4-methylphenyl)sulfonyl]-5-oxo-2,3,4,5-tetrahydro-1H-1-benzazepine-4-carbonitrile (**C9**)*

Potassium *t*-butoxide (1.76 g, 15.7 mmol) was added to a solution of **3** (2.91 g, 7.81 mmol) in dry DMF (8.74 mL) at an internal temperature of −10 °C. The mixture was then warmed to 0–5 °C and stirred for 2 h. Water was poured into the mixture at 0–5 °C, 2.2 mL of 37 % hydrochloric acid was added dropwise, and the mixture was stirred at 5 °C for 1 h. The resulting solid was isolated by filtration to give crude **C9**. A mixture of crude **C9** in methanol was stirred at reflux for 30 min, then cooled to 5 °C and stirred for 1 h. The resulting crystals were isolated by filtration and dried to afford **C9** as a white powder. mp: 152–153 °C. Yield: 77.2 %. ^{1}H NMR (300 MHz, DMSO-d_6): δ 2.09 (2H, m), 2.41 (3H, s), 3.39 (2H, br s), 7.31–7.58 (8H, m), 11.1 (1H, br s). IR (KBr): 3440, 2934, 2241, 1732 cm^{-1}. ^{13}C NMR (75 MHz, DMSO-d_6): δ 21.79, 26.59, 56.64, 82.16, 119.10, 127.46, 129.27, 130.60, 132.00, 132.20, 135.22, 136.92, 137.54, 143.94, 166.04.

Biological effects

*Blocking effects of **C9** on AVP-induced aortic ring contraction*

Animals were anesthetized with sodium pentobarbital (40 mg/kg of body weight; Holland de México) and underwent thoracolaparotomies. For each animal, the descending thoracic aorta was removed and placed in a Petri dish with Krebs–Henseleit (K–H) solution (NaCl 118 mM, KCl 4.7 mM, KH_2PO_4 1.2 mM, $MgSO_4{\cdot}2H_2O$ 1.2 mM, $CaCl_2{\cdot}2H_2O$ 2.5 mM, $NaHCO_3$ 25 mM, dextrose 11.7 mM and EDTA 0.026 mM). The adhering perivascular fat and connective tissue were carefully removed, and the segments were cut into rings of 3–4 mm in length. The endothelium of the rings was or not mechanically removed by inserting a rough surface wire into the vessel lumen. To measure tension changes, two triangle-shaped parallel steel strings were gently inserted into the ring, with one of the steel strings used to fix the ring in the bottom of the isolated organ chamber and the other connected to a tension transducer (TSD125C from BIOPAC). In turn, the transducer was connected to a MP150 data acquisition system from BIOPAC Systems Inc. in the following order: transducer, DA100C amplifier, universal interface module 100C, and a computerized system with the AcqKnowledge 3.8.1 program. The aortic rings were put into 10 mL isolated organ baths containing K–H solution at 37 °C and gassed with 95 % O_2 and 5 % CO_2. The initial tension was set at 4 g, and the rings were allowed to stabilize for at least 30 min to reach equilibrium. After the stabilization period, the aortic rings were contracted with AVP (0.1 μM) to prove the viability of the rings. Subsequently, an observation time was given to record the maximum contraction of the ring, which was then washed three times with K–H solution, and a new stabilization period was allowed before testing the drugs.

Influence of vascular endothelium on the maximum AVP-induced contraction

To discriminate between the contractile effects of AVP on V1aR of the VSM from the V2R-mediated vasodilator effects from the vascular endothelium, two studies were performed: (1) aorta rings with endothelium and (2) aorta rings without endothelium. For these experiments, the well-known V1aR peptide antagonist [(deamino-Pen^{1}, O-Me-Tyr^{2}, Arg^{8})-Vasopressin, Sigma V1880] was used. Assays started after the aortic ring viability test, and after the third H–K wash, the V1aR antagonist (10 μM) was added to the bath and was followed by a single pulse of AVP (0.1 μM). The percentage of AVP-induced maximum contraction was measured in the presence of V1aR antagonist. Finally, after three H–K washes, adrenaline (0.1 μM) was added to assess the rings' viability. Those rings that did not respond to an adrenaline pulse were considered non-viable and excluded from the study. These experiments allowed us to determine that in our conditions, vascular endothelium did not affect AVP-induced contractions (Fig. 5).

The AVP-induced (0.1 μM) VSM contraction in aortic rings with and without endothelium (Fig. 4) was blocked with the V1a antagonist (deamino-Pen1, O-Me-Tyr2, Arg8) Vasopressin, indicating that the vascular endothelium did not affect the vasopressor effect of AVP, whereas the V2-mediated endothelium vasodilator effect was not evident.

*Effect of **C9** on the contractility of vascular smooth muscle (VSM) from aortic rings*

Having established that the endothelium did not significantly affect the rings' contraction, the blocking effect of **C9** on AVP-induced contraction was assayed by testing several doses of **C9** (vide infra). Five experimental groups

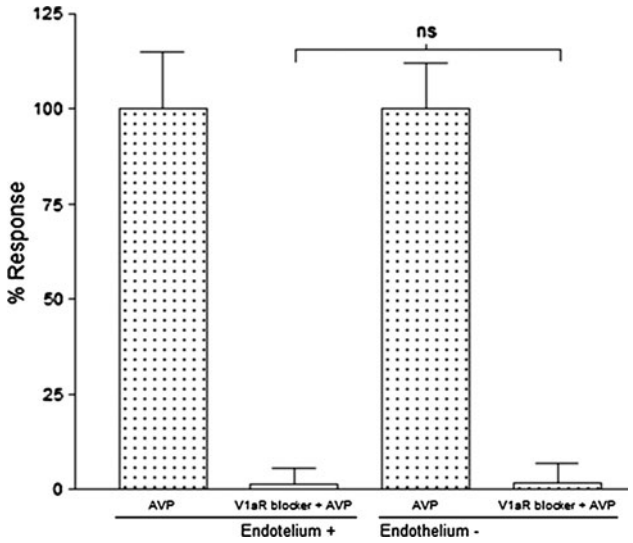

Fig. 4 Role of endothelial cells on aortic ring contraction in response to AVP. *First* and *second bars* represent *intact rings*, whereas the *third* and *fourth bars* represent *rings* without endothelium. No significant differences (NS) occurred between *first* and *third bars* nor between *second* and *fourth bars*. Values are the mean ± SEM of six experiments

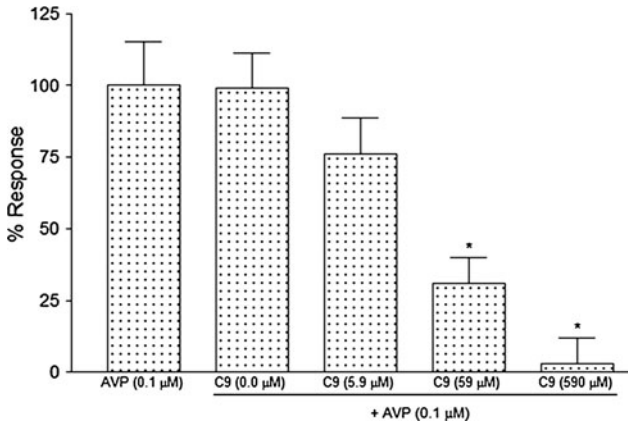

Fig. 5 Blocking effects of **C9** on AVP-induced aortic ring contractions. Note the concentration-dependent antagonism. $p < 0.01$: 59 and 590 μM versus AVP alone (vehicle for **C9**: DMSO. Vehicle for AVP: distilled water)

were formed: The first group received K–H solution and the second to fifth groups received increasing concentrations of **C9**—0.0, 5.9, 59, and 590 μM, respectively. DMSO was employed as a vehicle to reach a final concentration of 2 % in the bath. As described above, after the viability test and once the rings were washed, either K–H solution or **C9** was poured into the bath followed by a single AVP pulse (0.1 μM). The blocking effect of **C9** against ring contraction was expressed as the percentage of the AVP-induced maximum contraction. Finally, adrenaline (0.1 μM) was added to assess the rings' viability. The rings that did not respond to adrenaline-induced contractions were considered non-viable and discarded from the study.

Vasopressin (0.1 μM) induced the contraction of the aortic rings; this effect was inhibited in a dose-dependent manner by **C9**. The vasopressor activity of AVP was completely inhibited by **C9** at dose of 590 μM, whereas at 59 μM dose, the contraction was inhibited 70 %. At 5.9 μM dose, **C9** partially blocked (25 %) the vasopressor activity of AVP (NS vs AVP alone). Finally, the DMSO (vehicle) did not show any effect on the AVP-induced contraction (Fig. 5).

C9 blocks the antidiuretic effects of AVP in water-loaded rats

The water load test to evaluate the antidiuretic activity of AVP was originally developed by Dicker (1953) and subsequently modified by Bisset and Lewis (1962), Clark and Silva (1967), Bisset and Chowdrey (1984), and Yamamura *et al.* (1992). With minor changes, our protocol was as follows: Wistar rats were deprived of food for 18 h, but allowed free access to water. Before the experiment, the animals were loaded with a hypotonic saline solution (1.67 % glucose w/v and 0.3 % NaCl w/v, 3 % body weight) using a feeding tube. After full anesthesia (urethane 20 % w/v, 0.7 mL/100 g of b.w.), the trachea was cannulated for ventilation and a polyethylene intra-gastric catheter was inserted to deliver a constant administration of the hypotonic solution (5 mL each 30 min until the end of the experiment).

Subsequently, the carotid artery was cannulated for arterial blood pressure measurements using the MP150 data acquisition system from BIOPAC Systems Inc., the TSD104A blood pressure transducer, and the computerized system with the AcqKnowledge 3.8.1 program. The femoral vein and bladder were also cannulated for intravenous injections and urine collection, respectively. Urine samples were collected for 5-min periods throughout the experiment. Na^+ concentrations were assessed in each sample period using a Flame photometer 410 (Corning). The experiments were started when a constant urine flow was established, and the **C9** (100 μg/kg) was then intravenously administered, followed by a single dose of AVP (50 μU/kg/i.v.).

Intravenous injection of AVP (50 μU/kg of b.w.) in the water-loaded anesthetized rats induced a decrease in urine flow. After intravenous administration of **C9** (100 μg/kg b.w.), the antidiuretic action of exogenous AVP was inhibited (Fig. 6).

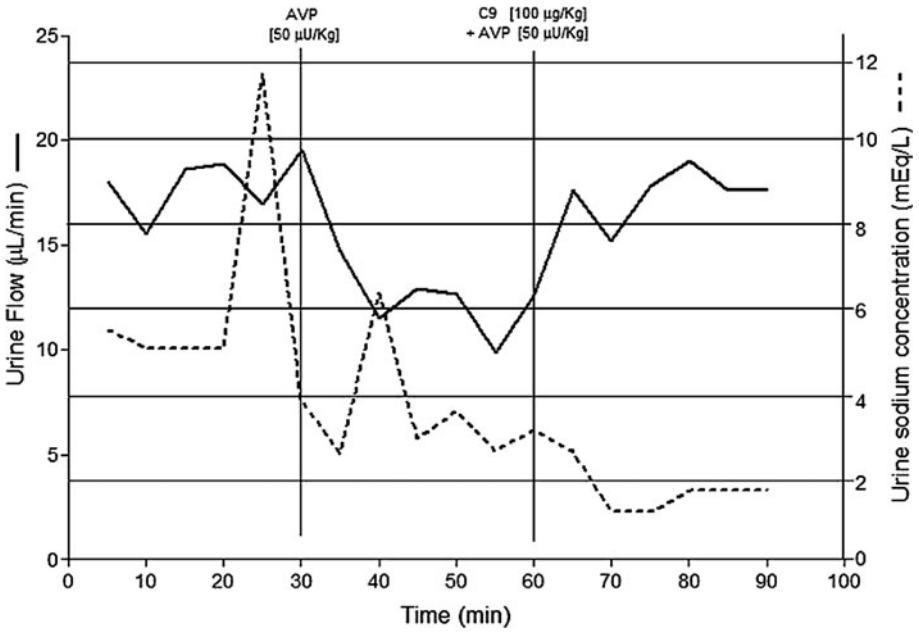

Fig. 6 Effects of AVP and **C9** on urine flow (*solid line*) and urine concentration sodium (*dotted line*) in rats subjected to a water load test. AVP (50 µU/kg) and **C9** (100 µg/kg) were administered intravenously. A typical trace from six experiments is shown

Data and statistical analysis

Biological data are presented as the mean ± SEM. The INSTAT 2 program for analysis of variance (ANOVA) was used to establish the significant differences between groups, and $p < 0.05$ was considered significant. Graphics were generated using PRISM 5.0.

Discussion

The synthetic route for **C9** was originally proposed by Tsunoda *et al.* (2004) as part of the synthesis pathway for Conivaptan. We adopted the same route of synthesis for **C9** with minor changes as follows: methyl 2-aminobenzoate was mixed with *p*-toluenesulfonyl chloride (TsCl) in pyridine and the reaction mixture was stirred at 25 °C for 11 h. To increase the yield, the reaction time was increased to 7 h; however, the yield was 10 % lower than the previous report, with a major loss in the filtering stage. To finalize the reaction, water at 5 °C was added into the mixture, stirring constantly for 1 h. The mixture was cooled at 5 °C to promote the formation of crystals of methyl 2-{[(4-methylphenyl)sulfonyl]amino}benzoate. Crystals were isolated by filtration and dried, with a yield of 82.2 %. The 4-chlorobutanenitrile, potassium carbonate, and potassium iodide were mixed with the *N*-tosyl benzoate from the previous reaction, and the mixture was dissolved in 2-butanone. The reaction mixture was stirred at reflux for 12 h and the system was allowed to cool to room temperature. It was necessary to add distilled water at 5 °C to favor the crystallization process of methyl 2-{(3-cyanopropyl)[(4-methylphenyl)sulfonyl]amino}benzoate. Next, modified-Dieckmann cyclization proposed by Tsunoda *et al.* (2004) was performed. This approach incorporates the use of *t*-BuOK instead of sodium hydride to circumvent the risk of hydrogen gas evolution as well as the need of purification to remove the oil used to disperse sodium hydride. After dissolving the methyl 2-{(3-cyanopropyl)[(4-methylphenyl)sulfonyl] amino}benzoate in DMF at −10 °C, *t*-BuOK was added to the reaction mixture. The mixture was constantly stirred for 2 h, and the temperature was maintained between 0 and 5 °C and water was slowly added. Concentrated HCl was added dropwise until a final volume of 2.2 mL, while maintaining constant stirring. After 1 h, the mixture formed a white precipitate (crude **C9**), which was dissolved in methanol and held at reflux for 30 min. The reaction mixture was then cooled at 5 °C to result in the formation of 1-[(4-methylphenyl)sulfonyl]-5-oxo-2,3,4,5-tetrahydro-1*H*-1-benzazepine-4-carbonitrile **C9** as a white precipitate that melted at 152–153 °C. The NMR spectrum of **C9** in DMSO-d_6 and its IR spectrum evidenced an OH in the enol form at position 5, which was also consistent with the previous report (Tsunoda *et al.*, 2004). Once **C9** was successfully synthesized, the compound was submitted for biological assays as described below.

To evaluate the antagonist effect of **C9** on V1aR, the aortic ring model was employed. It is known that in the activation of the endothelial V2 receptors by AVP, endothelial cells respond by releasing nitric oxide (NO), a vasodilator molecule with a short half-life (Okamura *et al.*, 1999). The aortic ring experiments showed that vascular endothelium did not play a significant role in the maximum

contraction of the AVP-induced VSM contraction (Fig. 4), possibly due to the small size of the rings and few endothelial cells to release NO molecules to induce relaxation. However, more experiments are needed to assess this assumption.

Once the influence of the endothelium on ring contraction was eliminated, subsequent experiments used only intact rings. The blocking activity of **C9** against AVP-induced aortic ring contraction was tested with different concentrations of **C9** (0.0, 5.9, 59, and 590 μM). The results showed that DMSO did not change the response to AVP, whereas several doses of **C9** caused a decreased response to AVP in a concentration-dependent manner. However, significant differences occurred only at the 59- and 590-μM doses of **C9** (Fig. 5). These results strongly suggest that **C9** has an antagonistic effect on AVP, possibly by acting on V1aR. That **C9** is responsible for this effect and not by a secondary metabolite is supported by the fact that in vitro there is no enzymatic mechanism to metabolize our compound. However, biological binding experiments are required to demonstrate the **C9**–V1aR interaction.

It is known that AVP is released when plasma osmolality is increased and/or plasma volume is reduced. Similarly, AVP release is inhibited when plasma osmolality is decreased and/or when plasma volume is increased (Jackson, 2006; Wagner and Braunwald, 1956). Animals subjected to the experimental water load test, in which an increased plasma volume was induced, experienced a decreased secretion of AVP (Jackson, 2006). Therefore, by measuring the changes in the urinary flow, we assayed the effects of **C9** as a blocker of the antidiuretic effect of exogenous AVP. Figure 6 shows the effects of AVP (50 μU) alone and AVP (50 μU) plus **C9** (100 μg/kg of **C9**) on the urinary flow rate. After a period of stabilization, the administration of AVP induced a decrease in the urinary flow (antidiuretic effect), which slowly returned to its basal level. The administration of AVP concurrent with **C9** at 60 min did not induce important changes in urinary flow. This indicates that **C9** blocked the antidiuretic effect of AVP. This result strongly suggests that **C9** may act as an AVP V2R antagonist.

Because urinary flow is also dependent on changes in the arterial blood pressure, we simultaneously measured the arterial blood pressure to discard AVP's vasopressor effects. The results showed that neither AVP alone nor AVP plus **C9** administrations affected the systolic, diastolic, or mean arterial blood pressures (results not shown). These results indicate that at the employed doses, the effects of AVP and **C9** were primarily on the kidney tubular system. Concerning the effects of AVP and **C9** on urinary sodium concentration, an unexpected transient increase in sodium concentration occurred with no changes in the urinary flow during the period of urinary flow stabilization (Fig. 6). Yamamura *et al.* (1992) demonstrated the aquaretic effect of OPC31260, a proved vasopressin antagonist that also contains a benzoazepinic ring into its structure, which can be considered a putative pharmacophore of vaptans (Contreras-Romo *et al.*, submitted), thus supporting the notion that the mechanism of **C9**'s aquaretic effect may be similar to that of OPC31260. These experiments strongly suggest that **C9** may possess an affinity for both V1a and V2 receptors. Additionally, we performed theoretical studies in order to explain the possible interaction mechanism of **C9** on these receptors.

Docking studies determined that **C9** has a binding free energy equal to −8.47 kcal/mol for V1aR. This high affinity of **C9** could be due to its chemical–structural similarity to vaptans, as mentioned above. The docking results suggest that the **C9** binding pocket in V1aR is constituted by residues such as T206, F207, P318, R214, S314, V217, Y216, S213, F189, G212, and W211 (Fig. 7). It is noteworthy that **C9** exhibits important π-π interactions with F207, W211, and Y216. However, it is possible that the interaction that governs the high affinity of **C9** on V1aR may be due to the hydrogen bond with R214, a fact that coincides with previous docking studies of the vaptans (Contreras-Romo *et al.*, submitted). For V2R, a binding free energy equivalent to −5.76 kcal/mol was determined. Results showed that the **C9** binding pocket on V2R is formed by residues including W200, P199, Q180, Q174, I209, Y124, M123, F287, Q291, and A294 (Fig. 8) making non-bonding interactions, such as a hydrogen bond between **C9** and the side chain of Q291 besides π–π interactions with F287, Y124, and W200 mainly. These binding poses are similar to those reported for Conivaptan on V2R (Giełdoń *et al.*, 2001).

According to these docking results, it is possible that **C9** reaches the V1aR and V2R active sites. This is due to **C9**'s

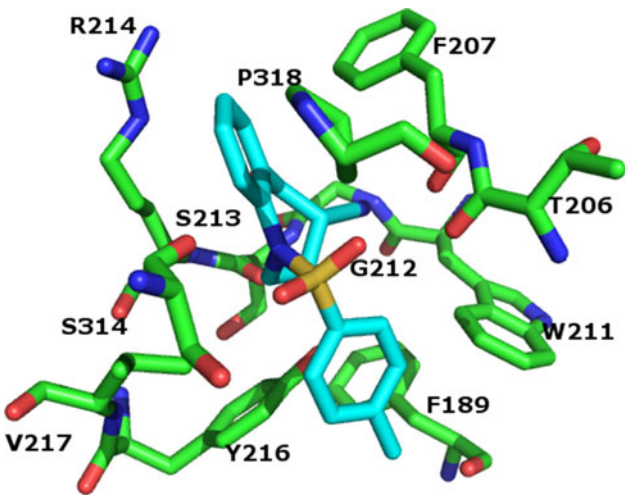

Fig. 7 V1aR amino acid residues involved in the binding of **C9**

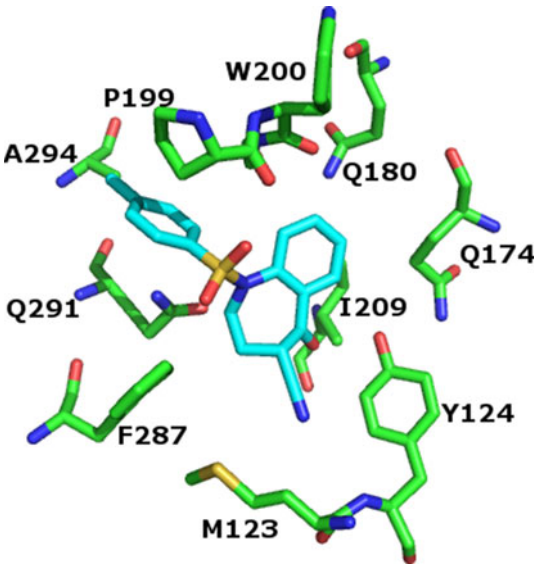

Fig. 8 V2R amino acid residues involved in the binding of **C9**

small size, allowing it to reach the bottom of the vasopressin receptor cavity. In addition, these ligands contain aromatic moieties that may facilitate their interaction with the cluster of amino acid residues that form the binding pocket. This hypothesis may be justified by the discovery of other proteins with the same binding pocket properties that have been found to stabilize aromatic ligands (Durán *et al.*, 2012).

Conclusions

The results of this work demonstrated that the chemical structure of **C9** is similar to that of most vaptans, whose benzoazepine core is a key moiety of this family of drugs. Docking studies of **C9** showed that this compound reaches the binding pocket of V1aR and V2R in the same manner as the vaptans, i.e., by interacting with key amino acids to recognize AVP. **C9** exhibited vasopressor and aquaretic effects when it was tested in experimental models of VSM contractility and diuresis. The results indicate that **C9** may be an important drug in the treatment of pathological diseases related to hydroelectrolyte imbalances, such as hyponatremia, the syndrome of inappropriate secretion of ADH, CHF, liver cirrhosis, and ascites. However, toxicological and experimental models of these diseases are needed to further probe these assumptions.

Acknowledgments We wish to thank to José Trujillo-Ferrara, Kalman Kovacs, and Rafael Camacho-Mejorado for their analysis, observations, and suggestions to the work and to Arturo Bustamante-Quezada, Juan Esparza-Valenzuela, Jesús Martínez-Hernández, Eleazar Luévano-Delgadillo, and María L. Rodríguez-Vázquez for their technical assistance. We thank CONACyT Grant 132353 and 204908 (IPN), CONACYT 62317 (UAA) and Grant PIBB-11-5 (UAA), Pfizer, ICyTDF (PIRIVE09-9), and COFAASIP/IPN for their financial support. We also wish to thank CONACYT for a scholarship to MCCR and fellowship to MMA.

Conflict of interest We also declare that there is no conflict of interest.

References

Barberis C, Durroux MB (1998) Structural bases of vasopressin/oxytocin receptor function. J Endocrinol 156:223–229

Bisset GW, Chowdrey HS (1984) A cholinergic link in the reflex release of vasopressin by hypotension in the rat. J Physiol 354:523–545

Bisset GW, Lewis GP (1962) A spectrum of pharmacological activity in some biologically active peptides. Br J Pharmacol 19:168–182

Clark BJ, Silva MRE (1967) An afferent pathway for the selective release of vasopressin in response to carotid occlusion and haemorrhage in the cat. J Physiol 191:529–542

Czaplewski C, Kazmierkiewicz R, Ciarkowski J (1998) Molecular modeling of the vasopressin V2 receptor antagonist interactions. Acta Biochim Pol 45(1):19–26

Dicker SE (1953) A method for the assay of very small amount of antidiuretic activity with a note on the antidiuretic titre of rats blood. J Physiol 122:149–157

du Vigneaud V, Gish DT, Katsoyannis PG (1954) A synthetic preparation possessing biological properties associated with arginine-vasopressin. J Am Chem Soc 76:4751–4752

Durán LA, Hernández MC, Hernández-Rodríguez M, Mendieta-Wejebe JE, Trujillo-Ferrara J, Correa-Basurto J (2012) Mapping myeloperoxidase to identify its promiscuity properties using docking and molecular dynamics simulations. Curr Pharm Des, in press

Giełdoń A, Kazmierkiewicz R, Slusarz R, Ciarkowski J (2001) Molecular modeling of interactions of the non-peptide antagonist YM087 with the human vasopressin V1a, V2 receptors and with oxytocin receptors. J Comput Aided Mol Des 15:1085–1104

Goldsmith SR (2005) Current treatments and novel pharmacologic treatments for hyponatremia in congestive heart failure. Am J Cardiol 95:14B–23B

Guyton AC, Hall JE (1999) Textbook of medical physiology, 9th edn. W.B. Saunders, Medina, pp 933–944

Hardman JG, Limbird LE (2001) Pharmacological basis of therapeutics, 10th edn. McGraw-Hill, New York, pp 789–944

Humphrey W, Dalke A, Schulten K (1996) VMD: visualmolecular dynamics. J Mol Graph 14:33–38

Jackson EK (2006) Vasopressin and other agents affecting the renal conservation of water. In: Brunton L, Lazo JS, Parker KL (eds) Goodman and Gilman's the pharmacological basis of therapeutics, 11th edn. McGraw-Hill, New York, pp 771–788

Laszlo FA, Laszlo F Jr, De Wied D (1991) Pharmacology and clinical perspectives of vasopressin antagonists. Pharmacol Rev 43:73–108

MacKerell AD, Bashford D Jr, Bellott M, Dunbrack RL Jr, Evanseck JM Jr, Field MJ, Fischer S, Gao J, Guo H, Ha DJ, Kuchnir K, Kuczera K, Lau FTK, Mattos C, Michnick T, Ngo T, Nguyen T, Prodhom B, Reither IWE, Boux M, Schlenkrich T, Smith R, Stote J, Straub M, Watanabe J, Wiorkiewicz-Kuczera D, Yin Karplus M (1998) All-atom empirical potential for molecular modeling and dynamics studies of proteins. J Phys Chem 102:3586–3616

Mah SC, Hofbauer KG (1987) Antagonists of arginine-vasopressin: experimental and clinical applications. Drugs Future 12:1055–1070

Martyna GJ, Tobias DJ, Klein ML (1994) Constant pressure molecular dynamics algorithms. J Chem Phys 101:4177–4189

Morris GM, Goodsell DS, Halliday RS, Huey R, Hart WE, Belew RK, Olson AJ (1998) Automated docking using a Lamarckian genetic algorithm and empirical binding free energy function. J Comput Chem 19:1639–1662

Mouillac B, Chini B, Balestre M, Elands J, Trumpp-Kallmeyer S, Hoflack J, Hibert M, Jard S, Barberis C (1995) Evidence for a major localization within transmembrane regions, the binding site of neuropeptide vasopressin V1a receptor. J Biol Chem 270(43):25771–25777

Okamura T, Ayajiki K, Fujioka H, Toda N (1999) Mechanisms underlying arginine vasopressin-induced relaxation in monkey isolated coronary arteries. J Hypertens 17:673–678

Philips JC, Braun R, Wang W, Gumbart J, Tajhhorshid E, Villa E, Chipot C, Skeel RD, Kalé L, Schulten K (2005) Scalable molecular dynamics with NAMD. J Comput Chem 26(16): 1781–1802

Ryckaert JP, Ciccotti G, Berendsen HJC (1977) Numerical integration of the Cartesian equations of motion of a system with constraints: molecular dynamics of n-alkanes. J Comput Phys 23(3):327–341

Schwieger I, Lautz K, Krause E, Rosenthal W, Wiesner B, Hermosilla R (2008) Derlin-1 and p97/valosin-containing protein mediate the endoplasmic reticulum-associated degradation of human V2 vasopressin receptors. Mol Pharmacol 3:697–708

Soriano-Ursúa MA, Trujillo-Ferrara JG, Correa-Basurto J (2010) Scope and difficulty in generating theoretical insights regarding ligand recognition and activation of the beta 2 adrenergic receptor. J Med Chem 53(3):923–932

Tahara A, Tomura Y, Wada K, Kusayama T (1997) Pharmacological profile of YM087, a novel potent vasopressin V1a-and V2-receptor antagonist, in vitro and in vivo. J Pharmacol Exp Ther 282:301–308

Thibonnier M, Coles P, Thibonnier A, Shoham M (2002) Molecular pharmacology and modelling of vasopressin receptors. Prog Brain Res 139:179–196

Tsunoda T, Tanaka A, Mase T, Sakamoto S (2004) A new synthetic route to YM087, an arginine vasopressin antagonist. Heterocycles 63(5):1113–1122

Wagner HW Jr, Braunwald E (1956) The pressor effect of the antidiuretic principle of the posterior pituitary in orthostatic hypotension. J Clin Invest 35:1412–1418

Yamamura Y, Ogawa H, Yamashita H, Chihara T, Miyamoto H, Nakamura S, Onogawa T, Yamashita T, Hosokawa T, Mori T, Tominaga M, Yabuuchi Y (1992) Characterization of a novel aquaretic agent, OPC-31260, as an orally effective, nonpeptide vasopressin V2 receptor antagonist. Br J Pharmacol 105:787–791

Zeltser D, Rosansky S, Van Rensburg H, Verbalis JG, Smith N (2007) Assessment of the efficacy and safety of intravenous Conivaptan in euvolemic and hypervolemic hyponatremia. Am J Nephrol 27:447–457

Zhang Y (2008) I-TASSER server for protein 3D structure prediction. BMC Bioinf 9:40